Journal of Power Sources 196 (2011) 133–139

Contents lists available at ScienceDirect

Journal of Power Sources

journal homepage: www.elsevier.com/locate/jpowsour

Cathode flooding behaviour in alkaline direct ethanol fuel cells

Y.S. Li, T.S. Zhao*, R. Chen

Department of Mechanical Engineering, The Hong Kong University of Science and Technology, Clear Water Bay, Kowloon, Hong Kong SAR, China

ARTICLE INFO

Article history:
Received 21 April 2010
Received in revised form 28 June 2010
Accepted 30 June 2010
Available online 13 July 2010

Keywords:
Fuel cell
Direct ethanol
Anion-exchange membrane
Water flux
Diffusion
Electro-osmotic drag

ABSTRACT

In an alkaline fuel cell, such as a direct ethanol fuel cell (DEFC), owing to the fact that water is consumed as a reactant at the cathode and the electro-osmotic drag (EOD) moves water from the cathode to the anode, a conventional conception is that the cathode flooding is unlikely. In this work, however, it is shown experimentally that cathode flooding also occurs in an alkaline DEFC, primarily because of the fact that the diffusion flux from the anode to the cathode outweighs the total water flux due to both the oxygen reduction reaction and EOD. More interestingly, rather than in acid electrolyte based fuel cells where the cathode flooding occurs at a high (limiting) current, in an alkaline DEFC the cathode flooding occurs at an intermediate current.

1. Introduction

Direct ethanol fuel cells (DEFCs) are more appealing than direct methanol fuel cells (DMFCs) because ethanol is less toxic than methanol and can be massively produced from agricultural products or biomass, in addition to the advantage of high specific energy. The performance of acid-membrane (typically Nafion®) based DEFCs is extremely low, however, and this is mainly because the electrochemical kinetics in acid media are sluggish. With the emergence of anion-exchange membranes (AEM), alkaline-membrane based DEFCs have recently been receiving ever-increasing attention [1–8], because the change in electrolyte from acid and alkaline can substantially speed up the electrochemical kinetics at both the anode and the cathode, even with Pt-free catalysts.

In developing alkaline DEFCs, efforts to date have been confined mainly to synthesis and characterization of materials, including membranes and catalysts, and mechanistic studies of the oxygen reduction reaction (ORR) and the ethanol oxidation reaction (EOR) [9–14]. This work is concerned with the problem of water flooding in the cathode of alkaline DEFCs. In acid-membrane based fuel cells, such as gas-hydrogen-feed proton exchange membrane fuel cells (PEMFCs) and DMFCs, water production at the cathode resulting from the ORR, which increases with current, along with water that permeates from the anode due to electro-osmotic drag (EOD) and possible diffusion, will make the liquid water accumulate at the cathode catalyst layer (CL) and the diffusion layer (DL). This is so-called cathode flooding, which resists the oxygen transport and thus lowers the cell performance. In particular, for a given cathode DL, flow-field and oxygen/air flow rate, cathode flooding will become more serious at high current densities, leading to a drastic drop in cell performance. Hence, tremendous effort has been devoted to water management in acid fuel cells to avoid the cathode flooding problem [15–19]. In an alkaline-membrane based fuel cell, such as a DEFC, owing to the fact that water is consumed as a reactant at the cathode and the EOD moves water from the cathode to anode, a conventional conception is that cathode flooding is unlikely [7,8]. In this work, however, the variation in the water flux from the cathode CL toward the DL of an alkaline DEFC with the current density is measured and it is found that the maximum water flux coincides with the cathode flooding that was visually observed through the transparent flow-field. This finding suggests that like in acid fuel cells, the cathode flooding also occurs in alkaline DEFCs.

2. Description of water transport in alkaline fuel cell

Consider a typical liquid-feed alkaline DEFC, as illustrated in Fig. 1, consisting sequentially of an anode flow-field, an anode DL, an anode CL, an anion-exchange membrane, a cathode CL, a cathode DL, and a cathode flow-field. Under discharging conditions, liquid water in the aqueous solution that is flowing in the anode flow-field is transported through the anode DL to the anode CL, along with that produced from the EOR, diffuses through the membrane to the cathode CL, where part of it reacts with oxygen to form hydroxide ions, and the remainder is transported through the cathode DL to

* Corresponding author. Tel.: +852 2358 8647; fax: +852 2358 1543.
E-mail address: metzhao@ust.hk (T.S. Zhao).

0378-7753/$ – see front matter © 2010 Elsevier B.V. All rights reserved.
doi:10.1016/j.jpowsour.2010.06.111

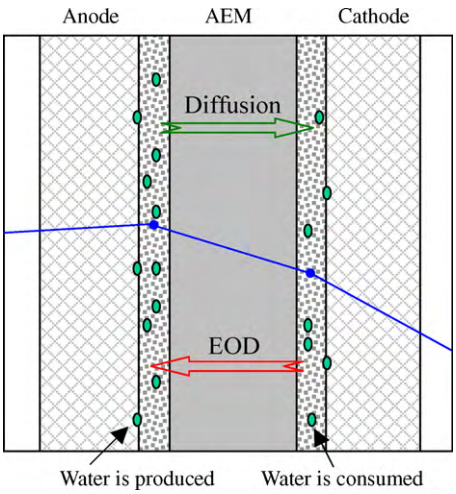

Fig. 1. Typical water distribution in alkaline DEFC.

the cathode flow-field. The water flux through the membrane due to diffusion, J_{diff}, can be expressed as:

$$J_{diff} = D\frac{c_{la} - c_{lc}}{\delta_m} \quad (1)$$

where D stands for the water diffusivity of the membrane; c_{la} and c_{lc} represent the liquid water concentrations at the anode and the cathode surfaces of the membrane, respectively; δ_m denotes the thickness of the membrane. Note that c_{la} increases with the rate of water generation due to the EOR at the anode, J_{EOR}, i.e.:

$$J_{EOR} = n\frac{i}{F} \quad (2)$$

where F is Faraday's constant; i is the current density; n denotes the ratio of the molar number between the produced water and the transferred electrons. Also note that c_{la} is affected by the water consumption rate due to the ORR at the cathode, J_{ORR}, i.e.:

$$J_{ORR} = \frac{i}{2F} \quad (3)$$

Under typical operating conditions, $c_{la} > c_{lc}$, meaning that the water flux by diffusion is from the anode to cathode. In other words, the water diffused from the anode is the sole source to maintain the ORR at the cathode if the oxygen/air supply is not humidified.

In addition to the water flux by diffusion from the anode to cathode, water can also be transported through the membrane by the EOD, J_{eo}, which can be determined from:

$$J_{eo} = n_d\frac{i}{F} \quad (4)$$

where n_d is the EOD coefficient of the membrane. Note that, in alkaline DEFCs, the hydroxide ions produced by the ORR travel through the membrane from the cathode to anode and hence the water flux by the EOD is in the opposite direction to that due to diffusion, i.e., J_{eo} is from the cathode to anode [20]. As a result, the net water flux from the anode to cathode (or the water-crossover flux through the membrane) is given by:

$$J_{wc} = J_{diff} - J_{eo} \quad (5)$$

It follows that the water flux from the cathode CL to the flow field, J, is:

$$J = J_{wc} - J_{ORR} \quad (6)$$

For convenience of description, the water flux from the cathode CL to the flow-field, J, is referred to as *the cathode water flux* hereafter. The above analysis suggests that the cathode water flux, J, varies with current density. It should be noted, however, that unlike in acid fuel cells, J may not increase monotonously with current density because the direction of water diffusion is opposite to that of the EOD.

Under steady-state operating conditions, the cathode water flux from the cathode CL is transported through the cathode DL to the flow-field, and eventually to the exit of the flow-field, i.e.:

$$J = J_{removal} \quad (7)$$

where $J_{removal}$ represents the water flux removed from the exit of the flow-field. Eq. (7) indicates that J can be determined by measuring $J_{removal}$ as described in the following section.

As an approximation, the steady-state cathode water flux can be expressed as:

$$J = \frac{c_{ccl} - c_{cff}}{k} \quad (8)$$

where k represents the overall mass-transport resistance that depends on the cathode DL and flow-field as well as the oxygen/air flow rate; c_{ccl} is the water concentration at the cathode CL; c_{cff} denotes the water concentration at the cathode flow-field. Eq. (8) indicates that, for a given design of cathode DL and flow-field at a fixed oxygen/air flow rate, c_{ccl} increases with the cathode water flux J. As c_{ccl} goes too high, the cathode will be flooded. Hence, cathode flooding occurs at high cathode water fluxes. In this work, the cathode water flux J was measured and the flow behaviour in the cathode flow-field was observed. With the data, a correlation between the cathode water flux J and the cathode flooding behaviour can be established.

3. Experimental

3.1. Fuel-cell setup

An in-house fabricated DEFC consisted of a membrane electrode assembly (MEA) with an active area of 2.0 × 2.0 cm, sandwiched between a pair of current-collectors. The MEA consisted of two single-sided electrodes and an anion-exchange membrane (A006, Tokuyama). The cathode electrode with non-platinum HYPERMECTM catalysts was provided by Acta. For the anode, the catalyst layer was fabricated in-house by a catalyst-coated substrate (CCS) method [5]. The catalyst ink was prepared by a method reported elsewhere [5] and then sprayed on a nickel foam plate (Hohsen Corp., Japan). The anode catalyst loading was about 2.0 mg cm^{-2} using synthesized PdNi/C [10]. The content of PTFE as a binder in the anode catalyst layer was maintained at about 5 wt.%. Finally, the MEA was formed by sandwiching the membrane between two electrodes that were attached with cell fixtures.

For convenience of temperature control with a heater, both the anode and cathode fixture plates were stainless-steel blocks. A single serpentine flow-field, having 1.0 mm rib width, 1.0 mm channel width, and 0.5 mm channel depth, was machined on one side of each fixture plate. In addition, to visualize two-phase transport behaviour in the cathode flow-field, a fixture made of transparent poly methyl methacrylate (PMMA) covered the current-collector plate.

3.2. Measurement instrumentation and test conditions

Experiments were performed with the test rig detailed elsewhere [18,21]. Tests of constant-current discharging behaviour of the DEFC were controlled and measured by an electric load system (Arbin BT2000, Arbin Instrument Inc.). At the cathode, air or 99.5% oxygen at ambient pressure with a flow rate from 10 to 200 standard cubic centimeters per minute (sccm) was supplied without

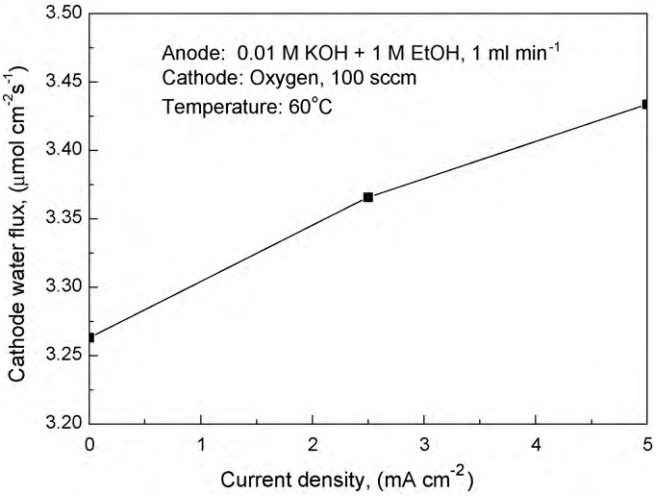

Fig. 2. Variation in cathode water flux with current density at 60 °C.

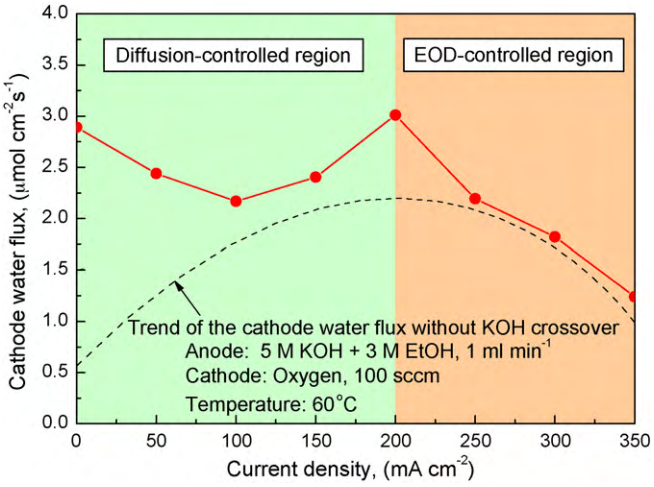

Fig. 3. Variation in cathode water flux with current density at 60 °C.

humidification. The flow rate of the gas was regulated and measured by a mass flow controller (Omega FMA-765A and FMA-767A), along with a multiple-channel indicator (Omega FMA-78P4). At the anode, the aqueous solution, containing ethanol and KOH, was fed by a peristaltic pump at a flow rate of 1.0 ml min^{-1}. In addition, before entering the fuel cells, the aqueous solution was preheated by electrical heating rods that were installed in the anode fixture plate. The cell operating temperature was measured with a thermocouple installed in the anode fixture plate.

3.3. Determination of cathode water flux

A water trap filled with anhydrous $CaSO_4$ (Dryerite®) was connected to the exit of the cathode flow-field to collect the water removed from the cell [18,22]. The cathode water flux was then determined by weighing the water collected in the trap over a specified time (ranging from 1.0 to 3 h) at a given current density. Thirty minutes were usually needed to achieve the steady-state condition at every water-collecting current density. The back pressures of both the anode and cathode electrodes were kept at atmosphere pressure to eliminate the influence of back pressures on water transport.

4. Results and discussion

4.1. General behaviour

Since the AEM employed in this work allows KOH to be transported from the anode to the cathode, KOH will be included in the water collected at the cathode exit. Therefore, prior to investigating the cathode water flux from the cathode CL to the flow-field under typical operating conditions (typically the required KOH concentration ≥1.0 M), the cathode water flux was first measured with an extremely low KOH concentration of 0.01 M to minimize the KOH crossover effect. The variation in the cathode water flux with current density is presented in Fig. 2. The cathode water flux increases with increasing current density. It is also noticed that the maximum current density in the *x*-axis is as low as 5 mA cm^{-2}, mainly because the electrochemical kinetics of the EOR in the low pH medium as a result of low KOH concentration are too sluggish, and result in an extremely low voltage when the current density is higher than 5 mA cm^{-2}. Nevertheless, Fig. 2 reflects the cathode water flux at low current density with a minimal effect of KOH crossover. The increase in cathode water flux with current density can be attributed to the increased water generation rate due to the EOR. A higher rate of water generation results in a higher water concentration at the anode CL, thereby increasing the water crossover through the membrane by diffusion. Therefore, the cathode water flux increases with current density. It should be pointed out, however, that under typical operating conditions with normally high KOH concentrations, the effect of KOH crossover will become significant. Moreover, as the water generation rate at the anode is low at low current densities, the impact of KOH crossover on the measured cathode water flux is the most serious at low current densities, but the effect will become weaker with an increase in current density.

Fig. 3 shows the variation in the cathode water flux with current density under typical operating conditions with the anode solution consisting of 3.0 M ethanol and 5.0 M KOH [21]. Unlike the cathode water fluxes with low KOH concentration as presented in Fig. 2,the data in Fig. 3 shows that there are two peaks in the cathode water flux-current density curve: the first peak occurs at zero current or at the open-circuit condition (OCC) with a water flux of 2.9 μmol cm^{-2} s^{-1}, while the second peak occurs at 200 mA cm^{-2} with a water flux of 3.0 μmol cm^{-2} s^{-1}. As mentioned earlier, since the rate of KOH crossover at the OCC is the highest, the first peak is actually caused by KOH crossover, rather than water crossover. Since the water generation rate due to EOR increases with current density, the water concentration at the anode CL increases accordingly, thereby lowering the KOH concentration at the anode CL and hence the rate of KOH crossover. In the meantime, the increased water concentration in the anode CL with increase in current density tends to enhance the cathode water flux. As a result, the effect of KOH crossover on the real cathode water flux becomes weaker with increasing current density. As projected, the real cathode water flux with the effect of KOH crossover eliminated should be the dashed curve shown in Fig. 3, which is lower than the measured data and increases with current density in the low current density region (<200 mA cm^{-2}). On the other hand, the water flux by the EOD, which is opposite to the water flux by diffusion, increases with current density. As a result, the combined effect of water flux to the cathode by diffusion and that to the anode by the EOD results in the second peak in Fig. 3. Hence this peak represents the highest cathode water flux, which occurs at a current density of 200 mA cm^{-2} under the particular test conditions used in this work. As indicated by Eq. (8), a high cathode water flux, *J*, means a high water concentration at the cathode CL, c_{ccl}. Since cathode flooding means that the water concentration at the cathode CL, c_{ccl}, is too high, the chance of cathode flooding is the highest at the higher cathode water flux.

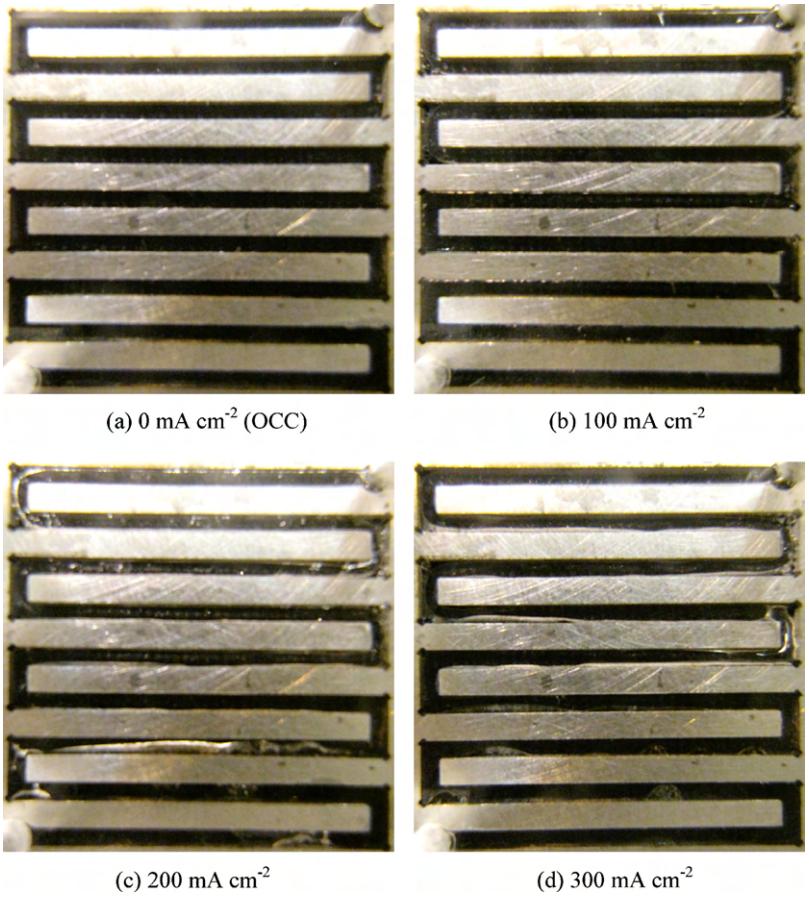

Fig. 4. Images of liquid water flow behaviour at different current densities at 60 °C. Anode: 3.0 M EtOH with 5.0 M KOH, 1.0 mL min^{-1}. Cathode oxygen flow rate: 100 sccm. Discharge current density: (a) 0 mA cm^{-2}, (b) 100 mA cm^{-2}, (c) 200 mA cm^{-2} and (d) 300 mA cm^{-2}.

To establish the correlation between the cathode water flux and cathode flooding, the water flow behaviour in the cathode flow-field was also observed. Fig. 4 shows images of the flow behaviour at different current densities, which were taken under the same operating conditions at that for measuring the cathode water flux shown in Fig. 3. The image in Fig. 4a shows that at the OCC a small amount of liquid water appears in the cathode flow-field. As the current density increases (see Fig. 4b), the amount of liquid water starts to increase in the cathode flow-field and the largest amount of liquid water is observed at 200 mA cm^{-2} (see Fig. 4c). When the current density is further increased to 300 mA cm^{-2} (see Fig. 4d), however the amount of liquid water in the flow-field becomes smaller. Apparently, the most flooded scenario shown in Fig. 4c is caused by the highest cathode water flux at 200 mA cm^{-2}. In summary, the visual study and the measured cathode water flux show that cathode flooding also occurs in an alkaline DEFC, but unlike in conventional PEMFCs and DMFCs, where cathode flooding occurs at the highest current density, in an alkaline DEFC, cathode flooding occurs at an intermediate current density, corresponding to the second peak of the cathode water flux in Fig. 3.

The cathode water flux was also measured at a lower operating temperature (40 °C) with a more concentrated ethanol solution (5.0 M) while other conditions were kept the same as those for the data shown in Fig. 3. The results are shown in Fig. 5. It can be seen that the variation in the cathode water flux with the current density exhibits a trend similar to that at 60 °C shown in Fig. 3. The highest cathode water flux occurs at a current density of 200 mA cm^{-2}. The visually experimental results shown in Fig. 6 also reveal that the highest cathode water flux and the largest amount of liquid water in the cathode flow-field (see Fig. 6b) appear at the same current density (200 mA cm^{-2}). This fact further confirms the correlation between the cathode water flux and cathode water flooding.

4.2. Relationships between cathode water flux and water fluxes by diffusion, EOD, EOR and ORR

As indicated by Eq. (6), the cathode water fluxes shown in Figs. 3 and 5 are the combined effects of the water fluxes by diffusion, EOD, EOR and ORR. The variation of the different water fluxes

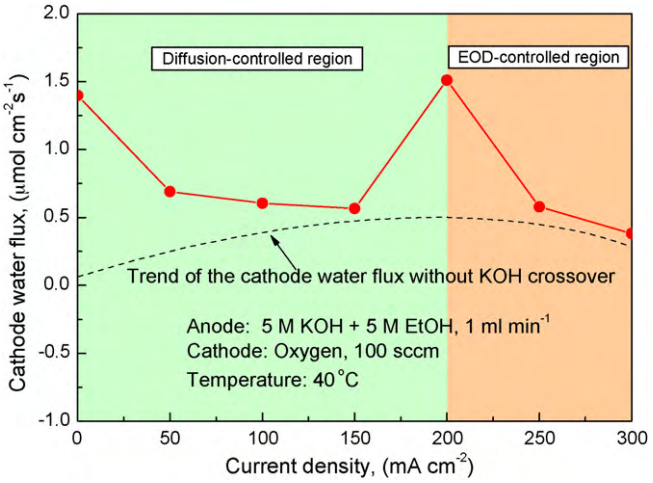

Fig. 5. Variation in cathode water flux with current density at 40 °C.

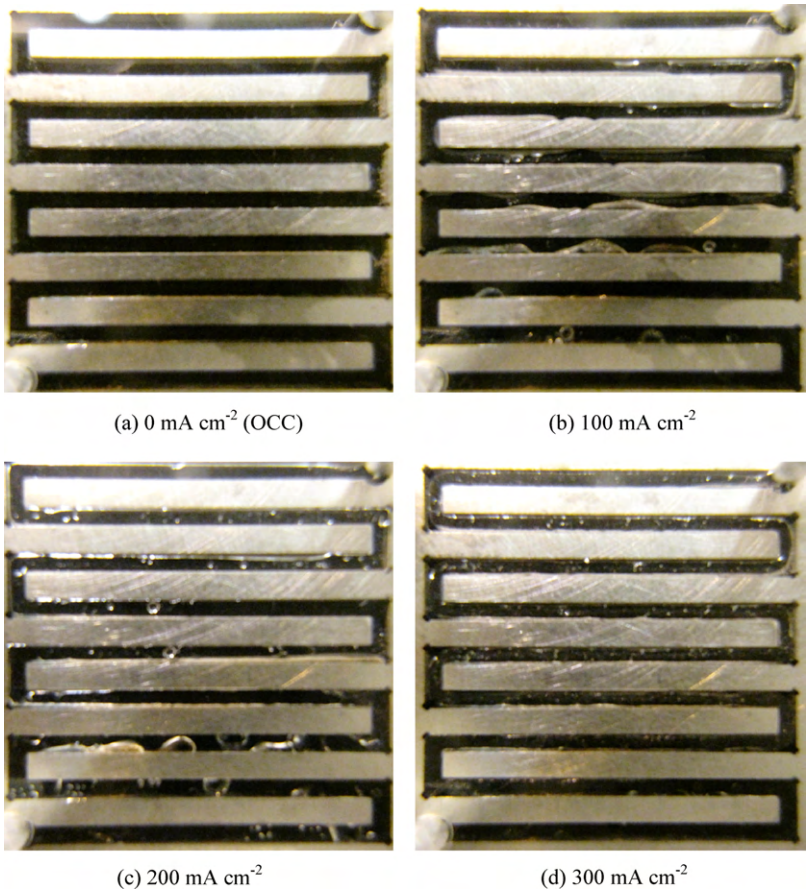

Fig. 6. Images of liquid water flow behaviour at different current densities at 40 °C. Anode: 5.0 M EtOH with 5.0 M KOH, 1.0 mL min^{-1}. Cathode oxygen flow rate: 100 sccm. Discharge current density: (a) 0 mA cm^{-2}, (b) 100 mA cm^{-2}, (c) 200 mA cm^{-2} and (d) 300 mA cm^{-2}.

with current density can be examined by referring to Fig. 7. First, it can be seen that the water flux by EOD, J_{eo}, which is determined from Eq. (4) with $n_d = 3.6$ [22], increases linearly with increasing current density, but the direction of the EOD in the alkaline DEFC is from the cathode to anode, i.e., opposite to that in acid DMFCs [18]. The water flux by the ORR, determined from Eq. (3), is also seen to increase with current density, but the magnitude is much smaller than that of the EOD. The water flux by the diffusion, J_{diff}, determined by combining Eqs. (5) and (6) with the measured cathode water flux, is seen to increase rapidly with increasing current density: the diffusion flux was 3.0 μmol cm^{-2} s^{-1} at 50 mA cm^{-2} and increased to 12.0 μmol cm^{-2} s^{-1} at 250 mA cm^{-2}. The reason for the rapid increase in the diffusion flux is that the water concentration at the anode CL increases with current density as a result of the increased water production by the EOR at the anode CL. Additionally, the water flux by the EOD from the cathode to anode also causes the water concentration in the anode CL to increase, thus further enhancing the water diffusion flux. As a result, the trade-

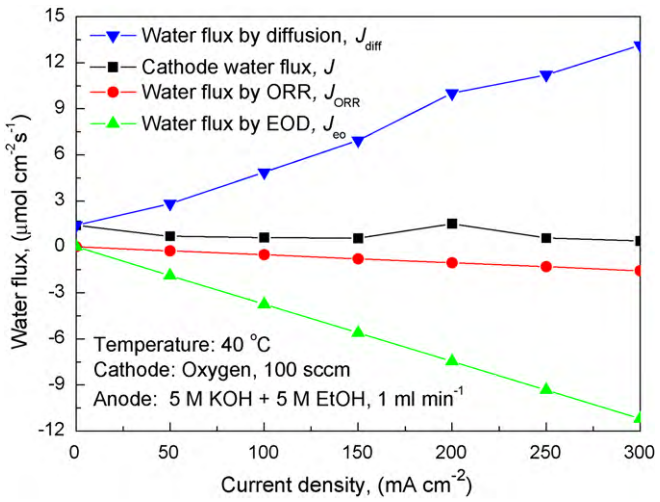

Fig. 7. Variation in water fluxes with current density at 40 °C.

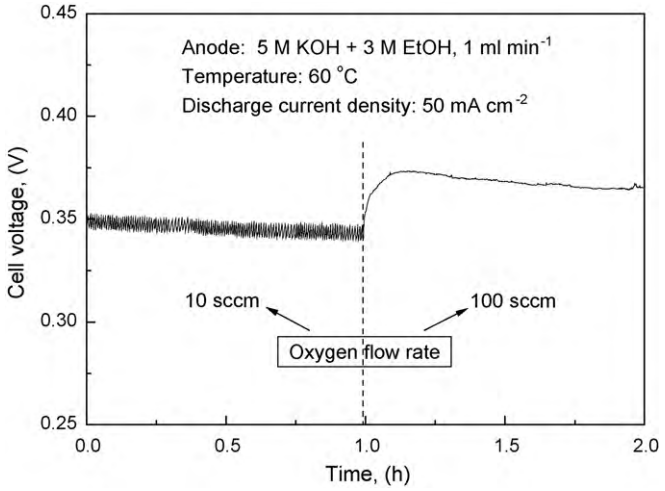

Fig. 8. Transient cell voltage at different oxygen flow rates at 60 °C.

(a) 10 sccm (b) 100 sccm

Fig. 9. Images of liquid water flow behaviour at different oxygen flow rates at 60 °C. Discharge current density: 50 mA cm^{-2}, anode: 3.0 M EtOH with 5.0 M KOH, 1.0 mL min^{-1}. Cathode oxygen flow rate: (a) 10 sccm and (b) 100 sccm.

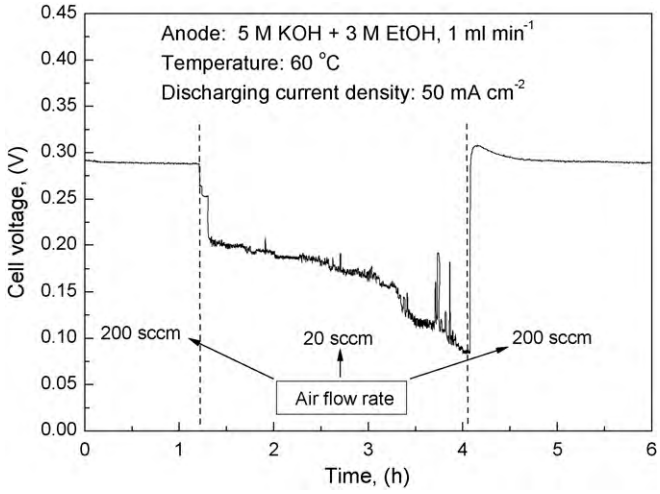

Fig. 10. Transient cell voltages at different air flow rates at 60 °C.

off between the water fluxes due to diffusion, EOD, EOR and ORR results in the cathode water flux first increasing and then decreasing with current density. This trend suggests that the cathode water flux is first dominated by water diffusion at low current densities (left region shown in Figs. 3 and 5) and then by EOD at high current densities (right region shown in Figs. 3 and 5), to form a cathode water flux peak at an intermediate current density. As indicated by Eq. (8), a higher cathode water flux means a higher water concentration at the cathode CL, that leads to more serious cathode flooding. Hence, in an alkaline DEFC operating under typical conditions, cathode flooding is more likely to occur at an intermediate current density that corresponds to a high cathode water flux.

4.3. Effect of water flooding on cell performance

The transient cell voltage with the oxygen flow rate varying from 10 to 100 sccm is presented in Fig. 8. The low oxygen flow rate (10 sccm) the cell voltage undergoes significant fluctuations, because the cathode flooding is more serious at low oxygen flow rates (see Fig. 9a, where liquid water almost covers the entire flow-field) and the periodic removal of liquid water from the flow-field causes the voltage to vary periodically. When the oxygen flow rate is increased to 100 sccm, however, the transient cell voltage becomes much more stable, as shown in Fig. 8. The reason why the voltage becomes stable at a higher oxygen flow rate is that the high oxygen flow rate facilitates the removal of excessive water. Consequently, the cathode flooding becomes less serious, as evidenced from Fig. 9b, where the liquid water only appears near the exit of the flow-field.

Experiments were also performed with air as the oxidant. The results are shown in Fig. 10. In the initial stage the higher air flow rate (200 sccm) results in a stable cell voltage. When the air flow rate is dropped to 20 sccm, however, the cell voltage experiences a sudden drop and significant fluctuations. As can be seen from Fig. 11a, the cathode flooding is rather serious at this low air flow

(a) 20 sccm (b) 200 sccm

Fig. 11. Images of liquid water flow behaviour at different air flow rates at 60 °C. Discharge current density: 50 mA cm^{-2}, Anode: 3.0 M EtOH with 5.0 M KOH, 1.0 mL min^{-1}. Cathode air flow rate: (a) 20 sccm and (b) 200 sccm.

rate. When the rate is increased back to 200 sccm, the water flooding shown in Fig. 11b became less serious and correspondingly, the cell voltage rises to the stable value, as shown in Fig. 10.

5. Concluding remarks

In an alkaline fuel cell, such as a DEFC, owing to the fact that water is consumed as a reactant at the cathode and the EOD moves water from the cathode to anode, a conventional conception is that the cathode flooding is unlikely. In this work, however, an investigation of the variation in cathode water flux from the cathode CL toward the DL with current density demonstrates that cathode flooding also occurs in an alkaline DEFC. Salient findings and conclusions are summarized as follows:

(1) At low current densities, the cathode water flux increases with the current density, as the forward water flux by diffusion outweighs the sum of the backward water fluxes by the EOD and ORR. When the current density became sufficiently high, however, the increased backward water fluxes by the EOD and ORR causes the cathode water flux to decrease with current density. As a result, there existed a peak cathode water flux that occurs at an intermediate current density.
(2) Visual observations of the flow behaviour in the cathode flow field reveals that cathode flooding coincides with the peak cathode water flux.
(3) It is shown that when the oxygen/air flow rate became sufficiently small, cathode flooding becomes more serious, and causes the cell voltage to decrease and discharging to become unstable.

Acknowledgements

The work described in this paper was fully supported by a grant from the Research Grants Council of the Hong Kong Special Administrative Region, China (Project No. 623008). The material support from Acta and Tokuyama is greatly acknowledged.

References

[1] Z. Ogumi, K. Matsuoka, S. Chiba, M. Matsuoka, Y. Iriyama, T. Abe, M. Inaba, Electrochemistry 70 (2002) 980–983.
[2] A. Verma, S. Basu, J. Power Sources 168 (2007) 200–210.
[3] C. Bianchini, V. Bambagioni, J. Filippi, A. Marchionni, F. Vizza, P. Bert, A. Tampucci, Electrochem. Commun. 11 (2009) 1077–1080.
[4] J.S. Spendelow, A. Wieckowski, Phys. Chem. Chem. Phys. 9 (2007) 2654–2675.
[5] Y.S. Li, T.S. Zhao, Z.X. Liang, J. Power Sources 190 (2009) 223–229.
[6] J.R. Varcoe, R.C.T. Slade, Fuel Cells 5 (2005) 187–200.
[7] E. Antolini, E.R. Gonzalez, J. Power Sources 195 (2010) 3431–3450.
[8] C. Bianchini, P.K. Shen, Chem. Rev. 109 (2009) 4183–4206.
[9] L.D. Zhu, T.S. Zhao, J.B. Xu, Z.X. Liang, J. Power Sources 187 (2009) 80–84.
[10] S.Y. Shen, T.S. Zhao, J.B. Xu, Y.S. Li, J. Power Sources 195 (2010) 1001–1006.
[11] R.C.T. Slade, J.R. Varcoe, Solid State Ionics 176 (2005) 585–597.
[12] F.P. Hu, P.K. Shen, J. Power Sources 173 (2007) 877–881.
[13] E.H. Yu, K. Scott, R.W. Reeve, Fuel Cells 3 (2003) 169–176.
[14] Z.X. Liang, T.S. Zhao, J.B. Xu, L.D. Zhu, Electrochim. Acta 54 (2009) 2203–2208.
[15] T.S. Zhao, C. Xu, R. Chen, W.W. Yang, Prog. Energy Combust. Sci. 35 (2009) 275–292.
[16] E. Peled, A. Blum, A. Aharon, M. Philosoph, Y. Lavi, Electrochem. Solid-State Lett. 6 (2003) A268–A271.
[17] H. Kim, J. Oh, J. Kim, H. Chang, J. Power Sources 162 (2006) 497–501.
[18] C. Xu, T.S. Zhao, J. Power Sources 168 (2007) 143–153.
[19] M. Neergat, A.K. Shukla, J. Power Sources 104 (2002) 289–294.
[20] T. Yamanaka, T. Takeguchi, H. Takahashi, W. Ueda, J. Electrochem. Soc. 156 (2009) 831–835.
[21] Y.S. Li, T.S. Zhao, Z.X. Liang, J. Power Sources 187 (2009) 387–392.
[22] Y.S. Li, T.S. Zhao, W.W. Yang, Int. J. Hydrogen Energy 35 (2010) 5656–5665.